Eugenol-Loaded Nanocarriers Exert Particle-Specific Adverse Effects to *Daphnia magna* Populations

Journal:	*Environmental Science & Technology*
Manuscript ID	es-2025-03624c.R1
Manuscript Type:	Article
Date Submitted by the Author:	26-Jun-2025
Complete List of Authors:	Brinkmann, Bregje; Leiden University, Environmental Biology Dupuis, Lan; Leiden University, Environmental Biology Houdijk, Sam; Leiden University, Center for Environmental Sciences Wattel, Pelle; Leiden University, Center for Environmental Sciences Salgado, Castor; Encapsulae SL Brunelli, Andrea; Ca' Foscari University of Venice, Department of Environmental Sciences, Informatics and Statistics Fernandez, Jose; Instituto de Ceramica y Vidrio, Electroceramic peijnenburg, willie; Leiden University, Vijver, Martina; Universiteit Leiden Centrum voor Milieukunde, Department of Environmental Biology

Eugenol-Loaded Nanocarriers Exert Particle-Specific Adverse Effects to *Daphnia magna* Populations

Bregje W. Brinkmann[1‡], Lan Dupuis[1‡], Sam Houdijk[1], Pelle Wattel[1], Cástor Salgado[2], Andrea Brunelli[3], José F. Fernández[4], Willie J.G.M. Peijnenburg[1,5,], Martina G. Vijver[1]*

[1] Leiden University, Institute of Environmental Sciences (CML), Leiden, 2333CC, The Netherlands

[2] Encapsulae SL, Castellón de la Plana, Spain

[3] Department of Environmental Sciences, Informatics and Statistics, Ca' Foscari University of Venice, Italy

[4] Instituto de Ceramica y Vidrio, ICV-CSIC, Madrid, Spain

[5] National Institute of Public Health and the Environment (RIVM), Center for Safety of Substances and Products, Bilthoven, 3720 BA, The Netherlands

* Corresponding author; E-mail: peijnenburg@cml.leidenuniv.nl

‡ These authors contributed equally

ABSTRACT

Nanocarriers provide promising prospects for the transition to more sustainable agrochemical practices. However, the unique release dynamics of their loaded chemicals raise concerns about potential adverse effects to non-target organisms. To address this, we compared the toxicity of bentonite and sepiolite nanocarriers loaded with the anesthetic/antibacterial chemical eugenol to the toxicity of pure eugenol. *Daphnia magna* was exposed to loaded nanocarriers, pure eugenol and bare nanocarriers. In acute immobilization tests, a 50%-effect concentration (EC_{50}) of 0.14 ± 0.01 mg eugenol·L^{-1} was derived for pure eugenol. Loading eugenol onto bentonite and sepiolite nanocarriers mitigated this acute toxicity, as indicated by respective EC_{50}-values of 0.48 ± 0.02 and 0.57 ± 0.07 mg eugenol·L^{-1}. In 12-day toxicity tests, similar concentrations of eugenol were released from both nanocarriers. For the first day of exposure, this temporarily reduced the swimming speed of daphnids. Moreover, in contrast to sepiolite nanocarriers, bentonite nanocarriers induced marked reductions in population growth. This reveals that nanocarriers exert particle-specific adverse effects to daphnid populations that cannot be predicted based on the toxicity of their individual constituents. We therefore plea to assess non-target effects of the complete nanocarrier system, including the carrier and its loading, before allowing these products on the market.

SYNOPSIS: Nanocarriers exert non-target effects to daphnid populations which depend on interactions between the bare nanocarrier, its chemical loading and biota.

KEYWORDS: advanced materials; nanocarriers; crop protection products; environmental safety; automated video tracking

INTRODUCTION

Advances in nanotechnology have led to the creation of nanocarrier systems to tackle modern challenges in medicine, agriculture, food and energy supply.[1,2] These systems, as defined by Gressler et al.,[3] include 'any material, material combination, chemical substance, compound, or structure with at least one dimension smaller than 1000 nm, capable of encapsulation or binding an active ingredient, aiming, among other things, to protect, disperse, transport, or sustain the release of the active ingredient and thereby enhancing its efficacy and/or safety'. For agricultural applications, nanocarriers complement other nano-enabled solutions in which the active ingredient (AI) is applied in a nanoform (e.g., metal oxides nanoparticles).[4] Crucially, nanocarrier crop protection products aim for a targeted and sustained exposure over time, employing the known efficiency of conventional pesticides combined with the inherent properties of nanomaterials to modulate the release of the AI.[5-7] This can be achieved through various designs, including the covalent binding or electrostatical attachment of the AI onto the surface of the carrier material, the adsorption of the AI into pores or in between branches of nanostructures like nanosponges or nanodendrimers, or by encapsulating the AI into capsules, such as nanoliposomes, empty pollen, virus capsids, or spore shells.[3] Owing to their lower effective dose and lower required application frequency, these systems have been suggested to decrease the environmental burden of pesticides.[8]

Nanocarriers have been proven to be more efficient in managing pests than metal-based nanoformulations and conventional agrochemicals in both lab and field-based experiments.[4] Additionally, a growing body of work indicates that pesticide-loaded nanocarriers may have equal or lower acute toxicity towards non-target species as compared to conventional analogues.[9-11] However, the very properties that make nanocarriers appealing, also raise questions about their potential toxicity to the environment.[12-14]

Most toxicity studies for nanocarriers are performed based on standardized acute toxicity tests, which do not capture the dynamic fate that is known for the release of the AI from nanocarriers.[15-18] Environmental conditions, including the pH, ionic strength, and presence of biomolecules, can influence the fate and behavior of nanocarrier systems.[19] For example, high ionic strength and the formation of biomolecular coronae can enhance the agglomeration of nanocarriers, whilst low pH and reducing redox conditions can promote the degradation and release of the AI from nanocarriers. To be able to capture the effects of slowly released chemical loadings from newly developed nanocarrier systems, fate and toxicity data need to be integrated over relevant timespans, and under realistic environmental conditions, as shaped by non-target biota. Without such understanding, there is a risk that nano-enabled pesticides which are applied to agricultural fields and unintendedly enter surface waters, will induce adverse effects to a wide range of aquatic species.[20-22]

In view of these considerations, we investigated how the toxicity of nanocarrier systems relates to the toxicity of the released AI, by characterizing the fate and toxicity of the released AI to the aquatic non-target organism *Daphnia magna*. We focus on different nanoclay carriers loaded with

a clove essential oil (CEO) extract, with the aim to determine 1) whether the long-term impacts induced by the nanocarriers can be extrapolated from their acute toxicity; and 2) whether those effects are fully driven by the AI, or depend on the nano-component. Nanoclays offer a versatile platform for the development of nanocarriers due to their biocompatibility, low toxicity, and cost-effectiveness.[23-25] The main AI of the CEO-loading is eugenol ($C_{10}H_{12}O_2$; 4-allyl-2-methoxyphenol), which is commonly used in the food and feed industry and in fisheries as an additive and an anaesthetic.[26,27] Eugenol additionally exhibits wide range-of-action pesticidal and antibacterial properties.[28-30] However, eugenol degrades quickly in the aquatic environment as a result of photooxidation.[31] The clay-based nanocarriers can delay this rapid degradation through the retarded release of adsorbed eugenol, thereby enhancing/extending the duration of the potential adverse effects of eugenol to aquatic organisms.

In the present study, we compared the toxicity of two different nanocarriers to *Daphnia magna* neonates and populations: a layered bentonite nanocarrier, and a fibrous sepiolite nanocarrier, both of which were loaded with CEO. The crustacean *D. magna* was selected as test species in view of its sensitivity to a large range of compounds, including the AI eugenol[32,33] and bare nanocarriers[34]. Automated tracking software was employed to track the survival, reproduction and swimming speed of daphnids from populations that were exposed to eugenol in its pure form, and to each of the nanocarrier systems. Quantification of actual concentrations of released eugenol in these tests revealed that both nanocarriers were applied at equivalent concentrations of released eugenol in the exposure medium. Owing to this equivalent dosing, the comparison between effects of both

nanocarriers in the present study allows to evaluate how nanocarrier-specific characteristics can shape adverse effects to non-target organisms.

MATERIAL AND METHODS

Daphnia magna cultures

Daphnia magna were reared as per OECD 211 recommendations.[35] Stock cultures were maintained in Elendt M7 medium at 22 ± 1˚C with a 16 h : 8 h (light : dark) photoperiod cycle. The rearing medium was oxygenated continuously, and its pH was maintained in between 7 and 9. The cultures were fed *ad libitum* with live *Raphidocelus subcapitata* three times a week. Neonates obtained from the culture were tested twice a year for their sensitivity to K_2CrO_7.[36] The results of this reference test complied with ISO 6341.2012 (0.6 mg·L^{-1} < $EC_{50,\ 24h}$ < 2.1 mg·L^{-1}).

Preparation of exposure media

Liquid eugenol (CAS 97-53-0; purity ≥ 99 %) was purchased from Sigma-Aldrich (Zwijndrecht, Netherlands). Bentonite and sepiolite nanocarriers were provided by SEPIOLSA (Minersa Group, Guadalajara, Spain) and consisted in layered and fibrillar nanoclay minerals. The nanocarrier were suspended in water media with a 10 % wt/wt of solids by a hand blender and stored for 24 hour before stirred with a Cowles type mixer (Dissolver SL-1 Heidolph RZR 2102) at 1200 rpm for 20 minutes and filtered with a 100 µm sieve. The slurries were transferred to a magnetic filter coupled

to a Xylen Flojet pump in order to remove iron-based impurities. The resulting suspensions were delaminated or defibrillated by using an ultra-turrax (IKA with rotor 8003300 T50) homogenizer and the suspension was heated up to 60°C. Both nanocarriers were loaded by the manufacturer with CEO. The CEO consisted of 16 % wt/wt caryophyllene (CAS 87-44-6), 84 % wt/wt eugenol and 0.02% carvacrol. CEO was loaded into the nanocarrier at a final concentration of 19-20 % wt/wt (for the bentonite nanocarrier) and 7-8 % wt/wt (for the sepiolite nanocarrier). In addition, the bentonite nanocarrier was stabilized with 1-2 wt/wt % fumaric acid, and the sepiolite nanocarrier was coated with 3-4 % wt/wt octadecylamine and stabilized with 2-3% wt/wt fumaric acid. The loaded nanocarriers were dried in a P-Selecta 2002972 DryBig oven at 80°C for 48 hours. Finally, the loaded nanocarriers were grounded with a Ultra Centrifugal Mill ZM300 (Retsch). In methanol extracts from both nanocarriers, 99.97 % eugenol, only 0.03% caryophyllene and no carvacrol were detected by gas chromatography coupled to mass spectrometry (GC-MS). Therefore, this study focused entirely on eugenol. Stock solutions and dispersions were prepared for 1) pure eugenol; 2) bare bentonite and sepiolite particles; 3) loaded bentonite and sepiolite nanocarriers; and 4) combined treatments, consisting of bare nanocarrier suspensions, spiked with pure eugenol. From here on, the complete nanocarrier systems, including their loading, are simply referred to as ‘nanocarriers’, whilst the bare nanocarriers are specifically named ‘bare nanocarrier’ or ‘bare bentonite/sepiolite particles’.

To prepare the eugenol stock solution, eugenol was first dissolved in 96 % ethanol at 7.5 $g \cdot L^{-1}$ (v. eq.). Thereafter, the stock was diluted in Elendt M7 medium to reach a final concentration of 500 mg $eugenol \cdot L^{-1}$. The solution was vigorously stirred for 10 min using a magnetic stirrer. Stock

suspensions of both nanocarriers in their bare and loaded form were prepared at a final concentration of 1 $g \cdot L^{-1}$ in M7 medium. The suspensions were magnetically stirred for 60 min at 1300 rpm using a magnetic stirrer. For combined treatments, stock suspensions of bare bentonite and sepiolite nanocarriers were spiked with pure eugenol at a eugenol concentration of 19 % (wt/wt) and 6.9 % (wt/wt), respectively. These percentages correspond to the eugenol content in the loaded nanocarriers. Freshly prepared stocks were vortexed immediately prior exposure, and diluted to the exposure concentrations in M7 medium (Table 1).

Exposure characterization

Exposure media were characterized in terms of 1) the primary particle size and shape of bare and loaded nanocarriers; 2) the zeta potential and hydrodynamic of aggregates from loaded nanocarriers; 3) the released concentrations of eugenol, measured over the full exposure duration.

Primary particle size and shape were characterized by way of transmission electron microscopy (TEM). To this end, 10 µL of 10 $mg \cdot L^{-1}$ bare and loaded nanocarrier suspensions were transferred to copper-mesh grids. The grids were allowed to dry for at least 24 h. Thereafter, particles were imaged using a JEOL 1400 microscope (JEOL Ltd., Japan) operating at 120 kV and a JEOL 2100F operating at 200KV with a Field Emission Gun.

The hydrodynamic size and zeta potential were determined for loaded nanocarrier suspensions of the medium test concentration (Table 2) using a Zetasizer Ultra instrument (Malvern Panalytical, United Kingdom). For these measurements, the absorption value was set to 0.01, the reflection index was set to 1.5 for bentonite nanocarrier,[37] and to 1.52 for sepiolite nanocarrier.[38]

Bare and loaded nanocarrier suspension stability was in situ monitored by using a Turbiscan-lab-backscattering-stability-analyzer (Microtrac Formulaction, France).

Aqueous concentrations of eugenol were measured for all exposures by ultra performance liquid chromatography inductively-coupled plasma mass spectrometry (UPLC-ICP-MS). The instruments and settings that were used for these measurements are provided in the Supporting Information (Tables S2, S3, and S4).

Toxicity tests

The toxicity of eugenol, and the bare and loaded nanocarriers, was tested by way of acute and long-term toxicity tests.

Acute tests were conducted following the standard acute immobilization guideline of OECD.[36] Five biological replicates were used for all concentrations. Test concentrations were selected based on a range-finding test, and were aimed to include the lowest effect concentration, the 100 % effect concentration, and three intermediate concentrations. Concentrations for the bare nanocarriers were based on concentrations of the loaded nanocarriers, by accounting for the weight of the loaded AI. These nominal concentrations, ranging from 0-5 mg pure eugenol·L^{-1}, from 0-500 mg nanocarrier·L^{-1}, and from 0-640 mg bare nanocarrier·L^{-1}, are presented in comparison to actual concentrations of eugenol in the results section (Table 1). Five *D. magna* neonates (<24 h old) were transferred from the main culture to 50 mL beakers filled with 20 mL exposure medium. Following Annex 1 of the test guideline, immobilization rate was assessed after 24 and 48 h of exposure as the fraction of neonates that did not swim within 15 s after gentle agitation of the test

vessel. Daphnids were not fed, and the medium was not oxygenated during exposure. Dissolved oxygen and pH were monitored during the experiment. At each timepoint, 2 mL of the exposure medium was sampled and centrifuged at 15400 g for 5 min. An aliquot of the supernatant was transferred to a 1 mL-tube and kept in the dark at 4 ˚C for quantification of aqueous eugenol concentrations.

Long-term tests of 12 d were performed to investigate sublethal effects of the nanocarriers on *D. magna* populations. The exposure concentrations for this test were derived from acute test results, selecting concentrations corresponding to 20 % (low) and 40 % (medium) of the acute EC_{50}-value. In addition to the loaded nanocarriers, bare nanocarriers, pure eugenol, and a treatment consisting of bare nanocarriers spiked with pure eugenol at concentrations corresponding to the loaded product, were included. All nominal exposure concentrations are presented in comparison to actual exposure concentrations in Table 2 and Table S5. At the start of each test, 10 daphnids of 10 d-old were transferred to 500 mL beakers comprising the exposure media. These exposure media were not artificially oxygenated. Four replicates of each exposure treatment were included. From each beaker, 2 mL of exposure medium was sampled on a daily basis, and immediately centrifuged for 5 min at 15400×g. The supernatant of these samples was stored at 4 ˚C until quantification of actual concentrations of released eugenol. At the same timepoints, population growth and swimming speed were assessed. During the 12-d exposure, daphnids were fed daily with fresh *R. subcapitata* algae, providing 0.5 mL of an $8.7 \cdot 10^5$ algal cells·mL^{-1} to each population. Both pH and dissolved oxygen concentrations were monitored over the full duration of the experiment.

Automated daphnid tracking

The count and swimming speed of daphnids were determined by way of automated tracking on an almost daily basis from 0 to 12 days post-exposure, excluding weekend days (as specified in Table S1). The setup described by Bruijning et al.[39] formed the inspiration and starting point for the tracking procedure. In this section we describe what adjustments were made to the recording, image pre-processing and tracking phase, in order to differentiate daphnids from aggregates of algae and nanocarriers. Detailed settings for each of the phases can be found in the Supporting Information (Table S1).

Recordings of daphnid populations were made in transparent Plexiglas cuvettes. This allowed daphnids to perform their natural up- and downward swimming motion, and moreover resulted in the spatial separation of swimming daphnids and settling aggregates of algae and nanocarriers. The content of each exposure beaker was carefully poured into the cuvette, was placed in a black cardboard box, and illuminated from the right and left side (Figure S1). Next, aggregates of algae and nanocarriers were allowed to settle for 30 s, 2.5 min-recordings were made, and the content of the cuvette was carefully poured back into the corresponding exposure beaker.

Image sequences were generated using FFMPEG (v. 5.0.3). The sequences were trimmed to 30 s of footage from the center of each movie, and were cropped to the outlines of the cuvette using the FIJI distribution of ImageJ2 (v. 2.14.0).[40] A median filter with a 2 pixel-diameter was applied to reduce noise from small algae and nanocarrier aggregates.

Tracking was performed using the R package Trackdem (v. 0.7.2).[39] This package identifies moving objects by subtracting motionless pixels (i.e. the 'still background') from each frame of the image sequence. At three steps, we applied filters to differentiate daphnids from moving aggregates of algae and particles. First, identified particles (i.e. algae, nanocarriers and daphnids), were filtered based on their size and intensity using the *partIden* function. Next, a neural network was trained using the *testNN* function, to filter any remaining false detections. We note that, given the aim to differentiate algae and nanocarrier aggregates from daphnids, the neural network was trained based on a reference image sequence comprising both adult and neonates of *D. magna,* as well as intermediate levels of clay and algae. Thereafter, tracks were computed using the *trackParticles* function, and any tracks spanning less than half of the recording were excluded. This prevented tracking the same daphnid twice, and moreover ensured that tracks from large aggregates of algae or nanocarriers that settled to the bottom of the cuvette were omitted. The corresponding R script, detailed tracking settings, and recorded parameters and are included in the Supporting Methods and Tables (Table S1).

The quality of the acquired tracking data was assessed based on plots of all detected particles and particle trajectories (see Figure S2 for example plots). This revealed that tracking results that were recorded on day 8 and day 10 (bare bentonite, bare sepiolite and pure eugenol) needed to be omitted due to tracking issues. Additionally, incorrect tracks corresponding to settling nanocarrier aggregates or reflections of daphnids on the walls of the cuvette, were manually removed from the data of day 0, 1 and 2 of the experiment.

Daphnid swimming speed

The average swimming speed ($\bar{v}$) was calculated for the 10 adult daphnids that started populations following:

$$\bar{v} = \frac{\Delta s}{\frac{1}{FPS} \cdot (f_{end} - f_{start})} \quad (1)$$

where Δs is the sum of displacement between all consecutive frames of a track, *FPS* is the frame rate, and f_{start} and f_{end} are the numbers of the first and final frame of a track, respectively. Neonates were excluded from swimming speed analysis, because these swim faster than adults, and have been exposed to different concentrations of eugenol, depending on their time of hatching. A size threshold of 50 pixels (8.8 mm) was applied to achieve this.

Data analyses

Data analysis and visualization was performed in R (v. 4.4.1; www.r-project.org) using the packages 'car' (3.1-3), 'drc' (v. 3.0.1),[41] 'dplyr' (1.1.4), 'lme4' (v. 1.1—35.5), 'plotrix' (v. 3.8-4), 'readr' (v. 2.1.5), and 'stats' (v. 4.4.1). The mean and the standard error of the mean (SEM) are reported.

Concentration-response curves, decay curves and growth curves were fitted using the *drm* function. The 4-parameters log-logistic model was used to obtain concentration-response curves, the 4-parameters Weibull model was used to obtain decay curves, and the 4-parameters logistic model was used to obtain growth curves. EC_{50} concentrations and slopes were compared using F-tests of the drc-integrated *compParm* function. The area under the curve (AUC) was computed using the *integrate* function.

The hydrodynamic size and zeta potential of aggregates from bentonite and sepiolite nanocarriers was compared using a Welch Two Sample t-test. Replicate measurements were averaged prior to this comparison. The Shapiro-Wilk test for normality was applied to check if sizes and zeta potentials of both nanocarriers followed a normal distribution. Additionally, Levene's test was used to check if the variance of size and zeta potential measurements was equally spread across the bentonite and sepiolite nanocarrier types.

The final population size was assessed by comparing the total count of daphnids between each of the treatments, as listed in Table 2 and Table S5, on the final day of exposure using the one-way ANOVA test combined with Tukey's HSD post-hoc test. Five populations that collapsed following exposure to the bentonite nanocarrier, and eight populations that collapsed following exposure to the combined treatment at medium effect levels, were excluded from the analysis. The normality of model residuals was assessed by inspecting diagnostic plots, and using the Shapiro-Wilk test for normality. Additionally, the equal spread of variance across all treatments was verified using Levene's test.

The relationship between the swimming speed of adult daphnids and concentrations of aqueous eugenol measured at the start of exposure (Table 2 and Table S5) was tested in a mixed-ANCOVA design using the *lmer* function. To account for the repeated measurement of populations from the same beaker, beaker was included as the random effect. Results for exposure day 0, day 1 and day 2 were tested separately. Three tests were performed for each of these days. The first test included all populations that were exposed to the bentonite nanocarrier, pure eugenol and the control. The second test included all populations that were exposed to the sepiolite nanocarrier,

pure eugenol and the control. The third test included all populations that were exposed to bare nanocarriers, either with or without the addition of pure eugenol. In the latter test, the clay type of the bare nanocarriers (bentonite or sepiolite) was included as a second explanatory variable, omitting the insignificant interaction between clay type and aqueous eugenol concentration (i.e. 'speed ~ [aqueous eugenol] + clay type + (1|beaker)'). For all tests, the normality of model residuals was checked by inspecting histograms and QQ-plots, generated using the *qqnorm* function. Additionally, residuals were plotted against fitted values, to check if model residuals distributed equally across each of the compared eugenol concentrations. Finally, *p*-values were computed based on a Type III Analysis of Variance with Satterhwaite's method, using the *anova* function.

Data availability statement

Video footage and the trained neural network will be made publicly available via Zenodo once the manuscript has been accepted for publication.

RESULTS

Nanocarrier size and shape

The primary particle size and shape of the bentonite and sepiolite nanocarriers in their bare and loaded form was investigated by way of TEM microscopy (Figure 1 and Figure S3). The size of

aggregates of (loaded) bentonite and sepiolite nanocarriers was additionally studied by dynamic light scattering (Figure S4).

Bare bentonite particles and bentonite nanocarriers were flake-shaped, had a primary size averaging 142.5 ± 3.4 nm, and a length to width ratio of 1.6 ± 0.1 (n = 10; Figure 1A,B). Due to the low electron density of these layered type particles, individual bentonite particles were hardly discernible when aggregated. Smaller particles (10 – 35 nm diameter) with higher electron density could be observed in the form of dark aggregates (Figure S3A) and correspond to amorphous silica particles in the form of opal nanoparticles (an amorphous form of silica, $SiO_2 \cdot nH_2O$). Opal nanoparticles can form naturally in sedimentary environments where silica-rich solutions precipitate under low temperatures. The similarity of this contamination for the bare bentonite particles and bentonite nanocarriers, still allows us to assess the effects of the bentonite nanocarrier based on the comparison of both materials. No differences in the primary particle size and shape could be observed between bare bentonite particles (Figure 1A and Figure S3A) and bentonite nanocarriers (Figure 1B and Figure S3B). In the exposure medium, the bentonite nanocarrier layered particles formed large aggregates with a hydrodynamic size and zeta potential averaging 2.9 ± 0.2 μm and -15.2 ± 0.8 mV respectively, according to DLS measurements, Figure S4. Although the primary particles of clays are laminar or fibrillar, their agglomerates do present a greater sphericity and the DLS measurements that correspond to agglomerates can be considered as an estimate of the size of said agglomerates. The aggregation of nanocarriers was enhanced by the fumaric acid encapsulant presence.

Bare sepiolite particles and sepiolite nanocarriers were needle-like shaped, with a length-to-width ratio of 23.5 ± 0.4 (n = 50; Figure S3C,D). The length of individual particles was highly heterogeneous and ranged from 20 nm to 5 µm. In contrast to the bentonite nanocarrier, essential oil was clearly visible as droplets on and around the needles of the sepiolite nanocarrier (Figure 1D). While the zeta potential of the sepiolite nanocarrier was significantly lower than that of bentonite nanocarrier, averaging -20.7 ± 0.9 mV (t = 4.6, df = 4.0, p = 0.01), sepiolite suspensions present larger aggregates than bentonite suspensions, with an average hydrodynamic size of 12.9 ± 5.2 μm, Figure S4. Due to the large spread in aggregate sizes, this mean size was not significantly different from the mean aggregate size for the bentonite nanocarrier (t = -1.9; df = 2.0; p > 0.05). We furthermore note that we did not observe any peaks in the size distributions of both nanocarriers that correspond to the monolayer or solvation layer thickness of these materials, indicating these remained unexfoliated and aggregated in the aqueous medium. Whilst additional measurements of the sheet thickness (e.g. by way of atomic force microscopy) are required to confirm this, these observations are in line with the TEM images (Figure S3), exclusively showing multi-layered sheets of bentonite flakes or sepiolite needles.

Regarding potential sedimentation dynamics, we did not observe significant differences in the mean hydrodynamic size of both the bentonite and the sepiolite nanocarrier following 1 and 2 days of exposure (Figure S4A,B). However, we observed a clear decrease in the derived count rate following 1 day of exposure for the bentonite nanocarrier (Figure S4C), and following 2 days of exposure for the sepiolite nanocarrier (Figure S4D).

By the contrary, in situ suspension stability studies (Figure S5) demonstrated that the higher hydrodynamic size of sepiolite bare and sepiolite nanocarrier resulted in higher sedimentation than bentonite bare and bentonite nanocarrier suspensions. This sedimentation behavior is in agreement with the lower values of zeta potential. However, it is worth notice that in both cases a lower transmittance was obtained for the loaded nanocarriers against its bare counterparts as an indicator of the presence of delaminated and defibrillated particles in the medium. This indicates that, while the bentonite nanocarrier appears to be somewhat more stable than the sepiolite nanocarrier, both nanocarriers settled over time. This indicates that, while the sepiolite nanocarrier appears to be somewhat more stable than the bentonite nanocarrier, both nanocarriers settled over time.

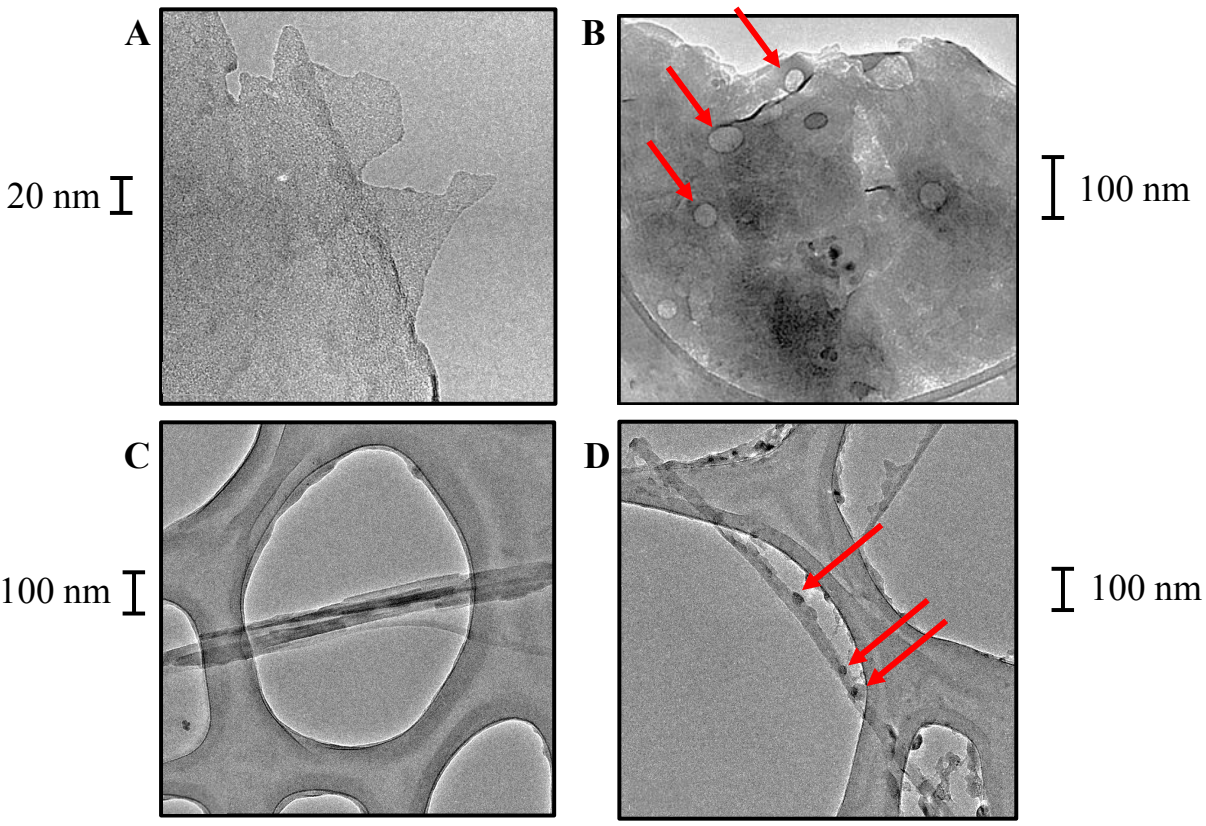

Figure 1. Transmission electron microscope micrographs of bare bentonite particles (A), the bentonite nanocarrier (B), bare sepiolite particles (C) and sepiolite nanocarrier (D). Red Arrows indicate CEO nanodrops in loaded nanocarriers.

Acute toxicity

The acute toxicity of bentonite and sepiolite nanocarriers was compared by way of the *Daphnia* acute immobilization test.[36] Nominal and actual exposure concentrations of eugenol in acute toxicity tests are compared in Table 1. While exposure to both the sepiolite nanocarrier and pure eugenol resulted in a maximal immobilization rate of 100% (Figure 2), a maximum immobilization rate of only 83.6 ± 6.9% was reached following exposure to the bentonite nanocarrier. These results indicate that the toxicity of the sepiolite nanocarrier was higher at high exposure concentrations than the toxicity of the bentonite nanocarrier. However, based on nominal nanocarrier concentrations (Figure 2A), a lower median effect concentration (EC_{50}) was obtained for the bentonite nanocarrier (83.6 ± 6.9 mg nanocarrier·L^{-1}) than for the sepiolite nanocarrier (130 ± 16.6 mg nanocarrier·L^{-1}; $t = 2.4$, $p = 0.02$). To investigate if this difference can be explained by the release of eugenol (the main AI of the loaded CEO), the toxicity of bentonite and sepiolite nanocarriers was next compared based on actual concentrations of released eugenol. Based on these actual concentrations of eugenol (Figure 2B), similar median effect levels were derived for the bentonite nanocarrier (0.48 ± 0.02 mg eugenol·L^{-1}) and the sepiolite nanocarrier (0.57 ± 0.07 mg eugenol·L^{-1}). The median effect level for pure eugenol was lower, averaging 0.14 ± 0.01 mg eugenol·L^{-1} ($t = 8.2$ and $t = -20.6$ as compared to bentonite and sepiolite nanocarrier, respectively;

$p < 0.001$). No immobilization was observed for daphnids that had been exposed to bare nanocarriers at concentrations corresponding to the highest test concentrations of the loaded nanocarriers (600 mg bare nanocarrier·L^{-1}). Combined, these results suggest that the acute toxicity of both nanocarriers is primarily driven by the release of eugenol into the medium.

Table 1. Comparison of nominal and actual concentrations of eugenol in acute toxicity tests. Total nanocarrier weights (nanocarrier + loading) are presented. Eugenol concentrations and release rates correspond to initially released eugenol concentrations. The total area under curves (AUC) was derived from aqueous eugenol concentration measured over the full exposure duration (Figure S6).

Treatment	nominal [nanocarrier] (mg·L^{-1})	nominal [eugenol] (mg·L^{-1})	actual [eugenol] (mg·L^{-1})	eugenol release rate (%)	AUC (mg·L^{-1}·2d)
pure eugenol	0.0	0.0	<LOD	NA	NA
	0.0	0.1	0.16 ± 0.001	NA	0.10
	0.0	0.25	0.29 ± 0.002	NA	0.17
	0.0	0.5	0.54 ± 0.03	NA	0.37
	0.0	1.0	1.59 ± 0.01	NA	0.72
	0.0	2.0	3.19 ± 0.04	NA	1.37
	0.0	5.0	5.80 ± 0.06	NA	2.05
bentonite nanocarrier	0.0	0.0	<LOD	NA	NA
	10	1.9	0.39 ± 0.006	20.5	0.18
	25	4.8	0.98 ± 0.001	20.4	0.37

	50	9.5	1.85 ± 0.02	19.5	0.70
	100	19	3.22 ± 0.02	16.9	1.07
	200	38	6.40 ± 0.09	16.8	2.24
	500	95	15.90 ± 0.07	16.7	6.18
sepiolite nanocarrier	0.0	0.0	<LOD	NA	NA
	10	0.7	0.24 ± 0.02	34.2	0.17
	25	1.7	0.57 ± 0.003	33.5	0.30
	50	3.5	1.05 ± 0.01	30.0	0.50
	100	6.9	2.09 ± 0.008	30.3	0.89
	200	13.8	4.15 ± 0.09	30.1	1.63
	500	34.5	9.70 ± 0.05	28.1	3.10

388 Abbreviations: CEO, clove essential oil; LOD, limit of detection; NA, not applicable.

389

390

391

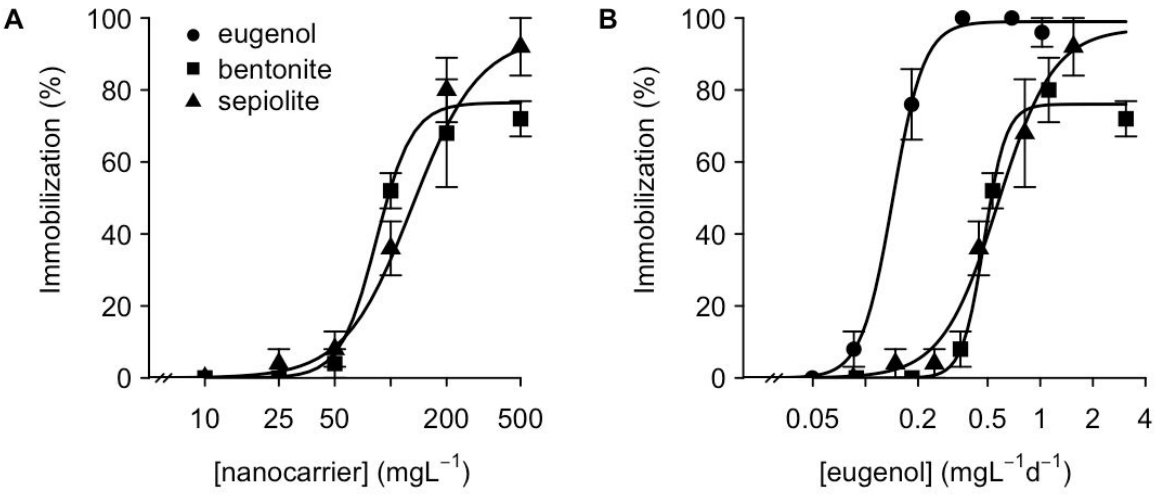

392

Figure 2. Fraction of immobilized *D. magna* neonates following 2 days of exposure to eugenol (circles), the bentonite nanocarrier (squares) and the sepiolite nanocarrier (triangles). Panel A presents concentration-response curves based on nominal nanocarrier concentrations. Panel B presents concentration-response curves based on the average actual concentrations of released eugenol per exposure day.

Population-level exposure dynamics

Based on the acute toxicity test, we subsequently investigated the effects of bentonite and sepiolite nanocarriers on *D. magna* populations at 20% and 40% of the acute toxicity EC_{50} values (Table 2).

Immediately following dispersion in Elendt M7, both nanocarriers released ~10-20% of their eugenol loading into the exposure medium (Table 2). The initial concentrations of eugenol did not differ between the bentonite (Figure 3A) and the sepiolite nanocarrier (Figure 3B). However, aqueous eugenol dissipated from the exposure medium in a nanocarrier-specific manner. For the bentonite nanocarrier, aqueous eugenol concentrations decreased gradually from the start of the experiment onwards, similar to the dissipation of eugenol without the addition of (bare) nanocarriers (Figure 3C; Table 2). In contrast, aqueous concentrations of eugenol remained stable in treatments with the sepiolite nanocarrier for the first 2 d of exposure, which was followed by a steeper decline of eugenol concentrations in the exposure medium. This behavior is in agreement with the higher sedimentation of the sepiolite nanocarrier and the low water solubility of the fumaric acid (0.63 g/100 ml) as encapsulant. The low solubility of the encapsulant constrained the

release of CEO nanodrops and this process is in turn impeded by the presence of aggregates. Thus, the larger hydrodynamic radius of the sepiolite aggregates acts as containers that release the CEO more gradually for sepiolite than for bentonite nanocarriers. Nevertheless, the total aqueous exposure to eugenol over 12 d of exposure, calculated as the area under the curve (AUC), was similar for both nanocarriers (Table 2). The concentration of eugenol in negative controls and bare nanocarrier treatments remained below the detection limit over the full duration of the experiment, confirming that these treatments were free of eugenol contamination.

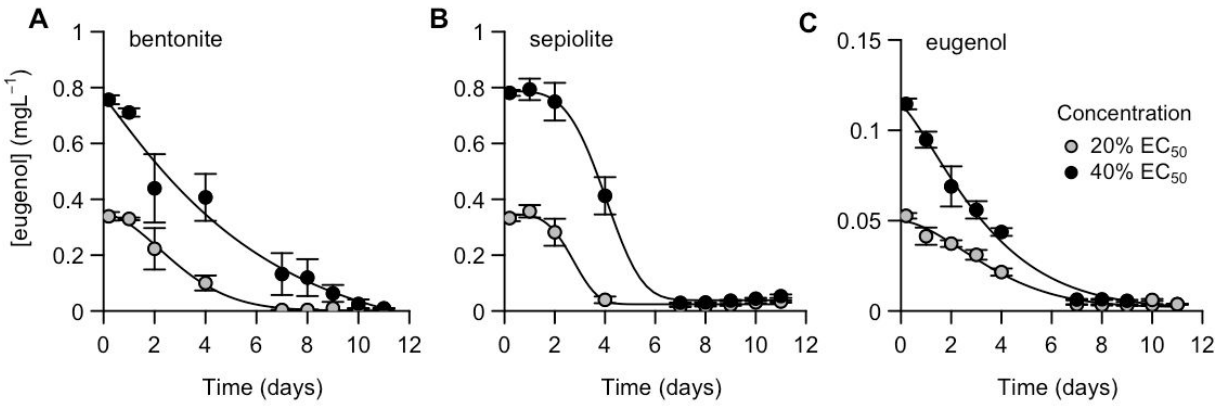

Figure 3. Aqueous eugenol concentrations in population-level tests for the bentonite nanocarrier (A); the sepiolite nanocarrier (B); and pure eugenol (C). Mean and SEM are presented ($n = 4$) for the low exposure concentrations (grey circles; 20% acute EC_{50} value) and medium exposure concentrations (black circles; 40% acute EC_{50} value). Decay curves were fitted based on the four-parameter Weibull model. Results for combined treatments of bare nanocarriers and eugenol are presented in Figure S6.

Table 2. Comparison of nominal and actual concentrations of eugenol in population-level tests. Total nanocarrier weights (nanocarrier + loading) are presented. Eugenol concentrations and release rates correspond to initially released eugenol concentrations. The total area under curves (AUC) was derived from aqueous eugenol concentration measured over the full exposure duration (Figure 3). Results for combined treatments are presented in Table S5.

Treatment	Exposure level	nominal [nanocarrier] ($mg \cdot L^{-1}$)	nominal [eugenol] ($mg \cdot L^{-1}$)	actual [eugenol] ($mg \cdot L^{-1}$)	eugenol release rate (%)	AUC ($mg \cdot L^{-1} \cdot 12d$)
bare bentonite	medium	23.5	0	< LOD	NA	NA
bentonite nanocarrier	low	17.0	3.4	0.34 ± 0.02	10.0	1.0
	medium	33.0	6.6	0.76 ± 0.02	11.2	3.1
bare sepiolite	medium	48.3	0	< LOD	NA	NA
sepiolite nanocarrier	low	26.0	1.8	0.33 ± 0.01	18.3	1.1
	medium	51.9	3.6	0.78 ± 0.01	21.7	3.3
pure eugenol	low	0	0.06	0.05 ± 0.002	NA	0.2
	medium	0	0.12	0.12 ± 0.003	NA	0.4

Abbreviations: CEO, clove essential oil; LOD, limit of detection; NA, not applicable.

When eugenol was mixed with the bare bentonite nanocarrier (Figure S6A) or the bare sepiolite nanocarrier (Figure S6C) at (nominal) concentrations corresponding to the loading of both nanocarriers, this resulted in much higher concentrations of eugenol in the exposure medium (Table S5). This fact confirms that the encapsulant plays an important role in the slow release of

CEO from the nanocarriers. As previously mentioned, the low solubility of fumaric acid slows the release of the nanodroplets, causing a prolonged effect of CEO in the medium. Conversely, if the CEO is only absorbed on the surface of the materials in the mixtures, the release occurs very rapidly due to its hydrophobic nature. The measured concentrations of eugenol were consistently lower than the nominally applied concentrations of eugenol for these treatments (Table S6), despite high resemblance of measured and nominal concentrations in pure eugenol treatments without bare particles (Table 2). Based on the assumption that the difference between measured and nominal concentrations of eugenol resulted from the adsorption of eugenol to bare particles, corresponding adsorption rates of 3.69 ± 0.13 % (wt/wt) and 1.10 ± 0.12 % (wt/wt) can be calculated for the bare bentonite and bare sepiolite nanocarrier, respectively. However, the high concentrations of aqueous eugenol in mixed treatments, compared to the concentrations of released eugenol from nanocarriers, complicate further comparison of the effects of these treatments. Therefore, results for the combined treatment are included in the Supporting Information.

Population-level effects

Immediately following exposure, treatments with both bentonite and sepiolite nanocarriers resulted in lower daphnid swimming speeds, proportionally to the released concentrations of eugenol (t = -3.0, df = 25.1; p = 0.005 for bentonite; t = -3.6, df = 19.3 and p = 0.002 for sepiolite; Figure 4A). Mixed treatments consisting of bare particles and eugenol, also resulted in slightly lower swimming speeds (t = -3.8, df = 19.7, p = 0.001), irrespective of the nanocarrier type (t = 0.22, df = 20.0, $p > 0.05$; Figure S8A). Except for loaded bentonite nanocarrier, these effects

dissipated over the next two days of exposure (Figure 4B-C; Figure S8B-C). In view of the dissipation of eugenol from the exposure medium at later timepoints, and the lethal effects of the bentonite nanocarrier at these timepoints, we did not analyze swimming speed from 3 days of exposure onwards.

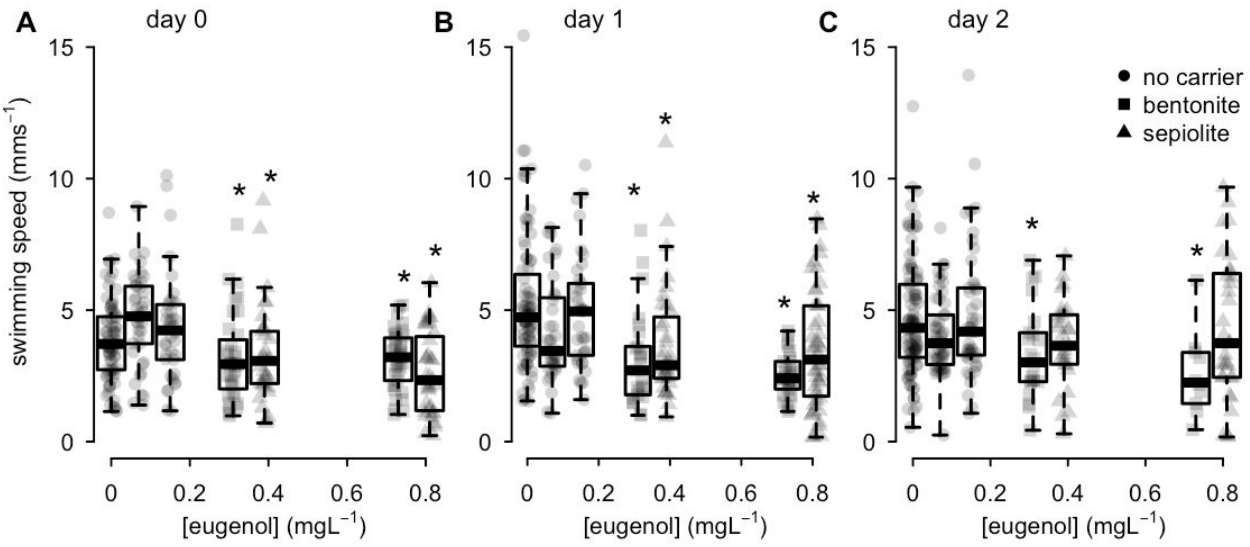

Figure 4. Swimming speed of *D. magna* individuals immediately following exposure (A), 1 day following exposure (B) or 2 days following exposure (C) to the bentonite nanocarrier (squares), the sepiolite nanocarrier (triangles) or pure eugenol (circles), as a function of the concentration of released eugenol. Results for bare particles, either applied with or without the addition of eugenol, are presented in Figure S6. Significant relationships between the released eugenol concentrations and swimming speed ($p < 0.05$) are indicated with an asterisk above the boxplots of the nanocarriers.

Compared to the effects of the nanocarriers on the swimming speed (Figure 4), much more profound effects were observed on the growth of daphnid populations over the 12-d exposure time in terms of daphnid count (Figure 5).

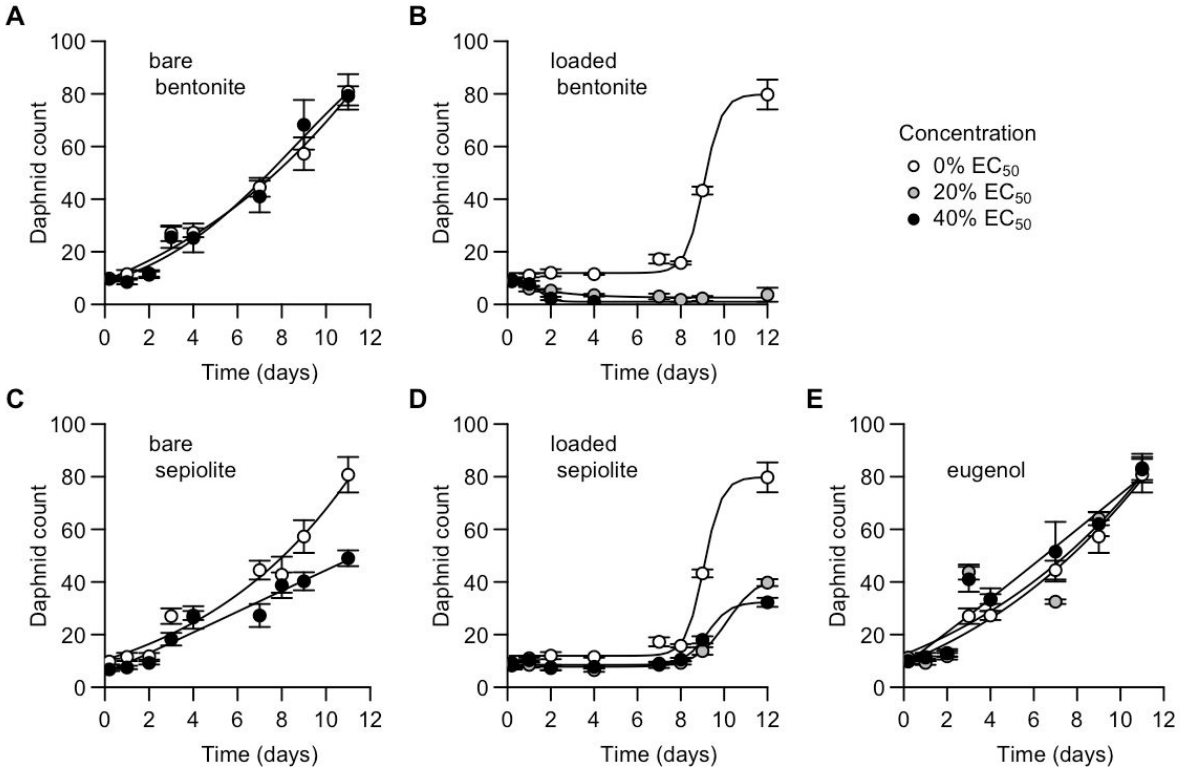

Figure 5. Growth of *D. magna* populations exposed to bare bentonite particles (A); the bentonite nanocarrier (B); bare sepiolite particles (C); the sepiolite nanocarrier (D); and pure eugenol (E). Mean and SEM are presented ($n = 4$) for the low exposure concentrations (grey circles; 20% acute EC_{50} value) and medium exposure concentrations (black circles; 40% acute EC_{50} value). Growth curves were fitted based on the four-parameter logistic model.

All populations started with an initial population count of 10 daphnids per exposure beaker. In the absence of nanocarriers and eugenol, these populations increased in 11 to 12 d to a final count

of 80 ± 4 individuals. Daphnid populations that were exposed to bare bentonite particles increased to a similar size of 79 ± 4 individuals at 11 d of exposure (Figure 5A). Remarkably, exposure to the bare sepiolite particles resulted in smaller population sizes, counting 49 ± 3 individuals at 11 d of exposure ($p < 0.0001$; Figure 5D).

When daphnids were exposed to the bentonite nanocarrier (Figure 5B), or applied to a mixture of bare bentonite particles and pure eugenol (Figure S7B), only 3 to 7 individuals survived to the end of exposure at the low exposure concentration. At the medium concentration, exposure to the bentonite nanocarrier even resulted in a full collapse of daphnid populations within 7 d. In contrast, when the sepiolite nanocarrier was applied (Figure 5D), daphnid populations still increased in size, albeit to lower population sizes than controls, counting 40 ± 1 and 32 ± 2 individuals at the low and medium exposure, respectively (Figure 5E; $p < 0.001$).

The effects of the mixed exposure to the bare sepiolite particles and eugenol on daphnid population growth were proportional to the added eugenol concentrations. Daphnid populations that were exposed to the low concentration of this mixture still reached a final population size of 38 ± 5 individuals at day 12, while populations that were exposed to the medium exposure fully collapsed within 7 d (Figure S7D). Exposures to pure eugenol did not impair population growth, irrespective of the exposure concentration, as assessed based on their final daphnid count, counting 83 ± 4 and 83 ± 5 individuals, respectively (Figure 5E).

DISCUSSION

A key aim for the development of nanocarrier systems for agricultural applications, is to modulate the release patterns of adsorbed or encapsulated chemical loadings to obtain more sustained and controlled exposure patterns. This nano-enabled tuning of exposure patterns requires a thorough assessment of chemical fate and toxicity towards unintendedly exposed non-target organisms.[18] The regulation of nanocarrier systems that are applied as crop protection products in Europe (EC No 1107/2009) is based on the assessment of the individual nanocarrier components (i.e. the active ingredient and the bare nanocarrier), where the active ingredient is additionally included in the REACH database of registered substances (EC No 1907/2006, article 15). However, our present study focusing on clay-based nanocarriers loaded with eugenol demonstrates that the longer-term effects of nanocarriers do not necessarily follow from the fate and effects of the released chemical loading and bare nanocarrier. As we discuss below, the prediction of longer-term adverse effects of nanocarriers therefore requires more thorough understanding of the behavior of nanocarriers in their environment.

In line with previous studies,[42-44] our acute toxicity tests indicate that nano-encapsulation mitigates the toxicity of the AI. Irrespective of the nanocarrier type, we observed a 3- to 4-fold decrease in the acute toxicity of eugenol upon loading. More specifically, we obtained 48 h-EC_{50}-levels of 0.14 ± 0.01 mg eugenol·L^{-1} for pure eugenol, of 0.57 ± 0.07 mg eugenol·L^{-1} for the sepiolite nanocarrier, and of 0.48 ± 0.02 mg eugenol·L^{-1} for the bentonite nanocarrier. These values are in the same order of magnitude of previously reported EC_{50}-levels,[45-47] ranging from 0.7 to 2 mg eugenol·L^{-1}.

In marked contrast to the acute toxicity tests, the population-level experiment showed profound differences between the toxicity of bentonite and sepiolite nanocarriers. At equivalent concentrations of released eugenol, the bentonite nanocarrier impaired population growth much more than the sepiolite nanocarrier. Similarly, while both nanocarriers initially impaired the swimming speed of *D. magna,* only daphnids that were exposed to the sepiolite nanocarrier recovered their swimming speed. Since no effects of bare bentonite nanocarriers could be observed, the higher toxicity of bentonite nanocarriers can only be attributed to interactions between the nanocarrier, its loading, and the exposed *D. magna*.

An important difference between the acute and population-level toxicity test, is the age of the daphnids that were used for these tests. Acute tests were executed with neonates, whilst population-level tests were executed with 10 d-old individuals who feed. *D. magna* can ingest bacteria and algae of 0.6 μm up to 40 μm in size,[48] although their ability to ingest 'hard' materials is more restricted. The largest ingestible polystyrene bead for daphnids was found to be 2-5 times smaller than the largest ingestible alga.[49] With respect to the nanocarriers, this could imply that daphnids can better ingest the smaller aggregates of the bentonite nanocarrier, than those of the sepiolite nanocarrier. Once ingested, nanocarriers are exposed to the different environmental conditions of the *D. magna* gut lumen, such as the low pH, high ionic strength, and presence of biomolecules,[50] which might affect the aggregation, residence time and degradation of the nanocarrier,[51] and can thereby influence the release of the AI. Therefore, the higher toxicity of the bentonite nanocarrier to daphnid populations could have resulted from the higher bioavailability of eugenol following its release from ingested nanocarriers.

Earlier, Vijver et al.[15] proposed to include the time-dependent fate of nanomaterials in the ecotoxicological evaluation of nano-enabled products. Our results reveal that this is particularly relevant for nanocarriers, as acute toxicity tests did not allow to accurately assess toxicity caused by the dynamic interactions between the bare nanocarrier, its loading, and biota. This implies that the hazard assessment for nanocarrier crop protection products must be conducted on a case-by-case basis, that is, for the loaded product rather than its individual constituents, and should include an evaluation of long-term effects. Additional *in vitro* tests should explicitly assess the influence of different environmental matrices, e.g. resembling the gut lumen of non-target organisms,[51] on the stability (OECD Test No. 318),[52] degradation (OECD Test No. 301),[53] and resulting release kinetics of the AI from nanocarriers.[54] Moreover, adjustments to dispersion protocols should be made to prevent preliminary degradation of nanocarriers by e.g. sonication procedures, resulting in the release of the AI prior to exposure. The first studies that investigate the toxicity of nanocarriers, thoroughly evaluated size as the particle-specific property.[55,56] Future directions should additionally include a detailed investigation of adsorption and desorption of the AI, and assessment of the impacts of interactions between nanocarriers and their environment on the fate and toxicity of nano-enabled products over time. This is necessary to fully assess their potential to replace conventional agrochemicals, and should therefore be included into routine testing prior to large-scale use.

ACKNOWLEDGEMENTS

This project has received funding from the European Union's ERC-consolidator grant agreement No 101002123 (granted to MGV) and the European Union's Horizon 2020 research and innovation program "SUNSHINE" (Grant Agreement number: 952924). We thank Gerda Lamers for acquiring TEM micrographs of the particles, Bas van Beusekom for providing the algae that were fed to *D. magna* cultures, and Marjolein Bruijning support with the use of Trackdem software.

ASSOCIATED CONTENT

The following files are available free of charge.

- Supporting Information including details on UPLC and tracking methods, figures and tables for the combined treatments with bare nanocarriers and pure eugenol, and additional DLS measurements.
- R environment file (.RData) including the trained neural network for daphnid tracking analysis.

REFERENCES

1. Gao, Y.; Liang, Y.; Zhou, Z.; Yang, J.; Tian, Y.; Niu, J.; Tang, G.; Tang, J.; Chen, X.; Li, Y.; Cao, Y. Metal-Organic Framework Nanohybrid Carrier for Precise Pesticide Delivery and Pest Management. *Chem. Eng. J.* 2021, *422*, 130143, DOI: 10.1016/j.cej.2021.130143

2. Sharma, S.; Perring, T. M.; Jeon, S.-J.; Huang, H.; Xu, W.; Islamovic, E.; Sharma, B.; Giraldo, Y. M.; Giraldo, J. P. Nanocarrier Mediated Delivery of Insecticides into Tarsi Enhances Stink Bug Mortality. *Nature Commun.* **2024**, *15(1)*, 9737, DOI: 10.1038/s41467-024-54013-7

3. Gressler, S.; Hipfinger, C.; Part, F.; Pavlicek, A.; Zafiu, C.; Giese, B. A systematic review of nanocarriers used in medicine and beyond – definition and categorization framework. *J. Nanotechnology,* **2025**, *23,* 90. DOI: 10.1186/s12951-025-03113-7

4. Wang, D.; Saleh, N. B.; Byro, A.; Zepp, R.; Sahle-Demessie, E.; Luxton, T. P.; Ho, K. T.; Burgess, R. M.; Flury, M.; White, J. C.; Su, C. Nano-Enabled Pesticides for Sustainable Agriculture and Global Food Security. *Nat. Nanotechnol.* **2022**, *17(4)*, 347–360, DOI: 10.1038/s41565-022-01082-8

5. Balaure, P.C.; Gudovan, D.; Gudovan, I. Nanopesticides: A New Paradigm in Crop Protection. In: New Pesticides and Soil Sensors, Elsevier, 2017, pp. 129 – 192. DOI: 10.1016/B978-0-12-804299-1.00005-9

6. Li, X.; Chen, Y.; Xu, J.; Lynch, I.; Guo, Z.; Xie, C.; Zhang, P. Advanced Nanopesticides: Advantage and Action Mechanisms. *Plant Physiol. Biochem.* **2023**, *203*, 108051, DOI: 10.1016/j.plaphy.2023.108051

7. Tang, Y.; Zhao, W.; Zhu, G.; Tan, Z.; Huang, L.; Zhang, P.; Gao, L.; Rui, Y. Nano-Pesticides and Fertilizers: Solutions for Global Food Security. *Nanomaterials* **2023**, *14(1)*, 90, DOI: 10.3390/nano14010090.

8. Ale, A.; Andrade, V. S.; Gutierrez, M. F.; Bacchetta, C.; Rossi, A. S.; Orihuela, P. S.; Desimone, M. F.; Cazenave, J. Nanotechnology-Based Pesticides: Environmental Fate and Ecotoxicity. *Toxicol. Appl. Pharmacol.* **2023**, *471*, 116560, DOI: 10.1016/j.taap.2023.116560

9. Campos, E. V. R.; Proença, P. L. F.; Oliveira, J. L.; Pereira, A. E. S.; De Morais Ribeiro, L. N.; Fernandes, F. O.; Gonçalves, K. C.; Polanczyk, R. A.; Pasquoto-Stigliani, T.; Lima, R.; Melville, C. C.; Della Vechia, J. F.; Andrade, D. J.; Fraceto, L. F. Carvacrol and Linalool Co-Loaded in β-Cyclodextrin-Grafted Chitosan Nanoparticles as Sustainable Biopesticide Aiming Pest Control. *Sci. Rep.* **2018**, *8(1)*, 7623, DOI: 10.1038/s41598-018-26043-x

10. Wu, T.; Fang, X.; Yang, Y.; Meng, W.; Yao, P.; Liu, Q.; Zhang, B.; Liu, F.; Zou, A.; Cheng, J. Eco-Friendly Water-Based λ-Cyhalothrin Polydopamine Microcapsule Suspension with High Adhesion on Leaf for Reducing Pesticides Loss. *J. Agric. Food Chem.* **2020**, *68(45)*, 12549–12557, DOI: 10.1021/acs.jafc.0c02245

11. Liang, Y.; Wang, S.; Jia, H.; Yao, Y.; Song, J.; Dong, H.; Cao, Y.; Zhu, F.; Huo, Z. Pectin Functionalized Metal-Organic Frameworks as Dual-Stimuli-Responsive Carriers to Improve the Pesticide Targeting and Reduce Environmental Risks. *Colloids Surf. B Biointerfaces* **2022**, *219*, 112796, DOI: 10.1016/j.colsurfb.2022.112796

12. Grillo, R.; Fraceto, L. F.; Amorim, M. J. B.; Scott-Fordsmand, J. J.; Schoonjans, R.; Chaudhry, Q. (2021). Ecotoxicological and Regulatory Aspects of Environmental Sustainability of Nanopesticides. *J. Hazard. Mater.* **2021**, *404*, 124148, DOI: 10.1016/j.jhazmat.2020.124148

13. Xu, Z.; Tang, T.; Lin, Q.; Yu, J.; Zhang, C.; Zhao, X.; Kah, M.; Li, L. Environmental Risks and the Potential Benefits of Nanopesticides: A review. *Environ. Chem. Lett.* **2022**, *20(3),* 2097–2108, DOI: 10.1007/s10311-021-01338-0

14. Eghbalinejad, M.; López-Cabeza, R.; Kotouček, J.; Grillo, R.; Koutný, M.; Bílková, Z.; Hofman, J. Effects of Three Tebuconazole Nanopesticides on the Survival of *Daphnia magna*. *Environ. Sci. Nano* **2024**, *11(3)*, 1044–1059, DOI: 10.1039/D3EN00673E

15. Vijver, M.G.; Zhai, Y., Wang, Z., Peijnenburg, W.J.G.M. Emerging Investigator Series: The Dynamics of Particle Size Distributions Need to be Accounted for in Bioavailability Modelling of Nanoparticles. *Environ. Sci. Nano* **2018**, *5*, 2473–2481, DOI: 10.1039/C8EN00572A

16. Valsemi-Jones, E.; Lynch, I. How Safe are Nanomaterials? *Science* **2015**, *350*, 388–389, DOI: 10.1126/science.aad0768

17. Hunt, N.; Kestens, V.; Rasmussen, K.; Badetti, E.; Soeteman-Hernández, L. G.; Oomen, A. G.; Peijnenburg, W.; Hristozov, D.; Rauscher, H. Regulatory Preparedness for Multicomponent Nanomaterials: Current State, Gaps and Challenges of Reach. *NanoImpact* **2025**, *37*, 100538. DOI: 10.1016/j.impact.2024.100538

18. Nederstigt, T. A. P.; Brinkmann, B. W.; Peijnenburg, W. J. G. M.; Vijver, M. G.. Sustainability Claims of Nanoenabled Pesticides Require a More Thorough Evaluation. *Environ. Sci. Technol.* 2024, *58*, 2163–2165, DOI: 10.1021/acs.est.3c10207

19. Manayath, D.; Travas-Sejdic, J.; Leitao, E.M.; Kah, M. Environmental and Human Risk Assessment of Polymer Nanocarriers: A Review on Current Analytical Challenges and Promising Approaches. *Environ. Sci.: Nano,* 2025, 12, 1079. DOI: 10.1039/d4en01033g

20. Schafer, R.B.; Van Den Brink, P.J.; Liess, M. (2011). Impacts of Pesticides on Freshwater Ecosystems, In: Ecological Impacts of Toxic Chemicals. *Bentham Science Publishers*, 2011, pp. 111–137, DOI: 10.2174/978160805121211101010111

21. Kah, M.; Kookana, R. S.; Gogos, A.; Bucheli, T. D. A Critical Evaluation of Nanopesticides and Nanofertilizers Against their Conventional analogues. *Nat. Nanotechnol.*, 2018, *13(8)*, 677–684. DOI: 10.1038/s41565-018-0131-1

22. Souza, De R. M.; Seibert, D.; Quesada, H. B.; De Jesus Bassetti, F.; Fagundes-Klen, M. R.; Bergamasco, R. Occurrence, Impacts and General Aspects of Pesticides in Surface Water: A Review. *Process Saf. Environ. Prot.* 2020, *135*, 22–37, DOI: 10.1016/j.psep.2019.12.035

23. Pinto, T. V.; Silva, C. A.; Siquenique, S.; Learmonth, D. A. Micro- and Nanocarriers for Encapsulation of Biological Plant Protection Agents: A Systematic Literature Review. *ACS Agric. Sci. Technol.* 2022, *2(5),* 838–857, DOI: 10.1021/acsagscitech.2c00113

24. Singh, G.; Ramadass, K.; Sooriyakumar, P.; Hettithanthri, O.; Vithange, M.; Bolan, N.; Tavakkoli, E., Van Zwieten, L.; Vinu, A. Nanoporous Materials for Pesticide Formulation and Delivery in the Agricultural Sector. *J. Contr. Release*, 2022, *343*, 187–206. DOI: 10.1016/j.jconrel.2022.01.036

25. Anjaneyulu, B.; Chauhan, V.; Mittal, C.; Afshari, M. Innovative Nanocarrier Systems: A Comprehensive Exploration of Recent Developments in Nano-Biopesticide Formulations. *J. Environ. Chem. Eng.* 2024, *12(5),* 113693, DOI: 10.1016/j.jece.2024.113693

26. Grush, J.; Noakes, D. L. G.; Moccia, R. D. The Efficacy of Clove Oil as an Anesthetic for the Zebrafish, *Danio rerio* (Hamilton). *Zebrafish* 2004, *1(1)*, 46–53, DOI: 10.1089/154585404774101671

27. Souza Valente, De C. Anaesthesia of Decapod Crustaceans. *Vet. Anim. Sci.* 2022, *16*, 100252, DOI: 10.1016/j.vas.2022.100252

28. Dorman, H. J. D.; Deans, S. G. Antimicrobial Agents from Plants: Antibacterial Activity of Plant Volatile Oils. *J. Appl. Microbiol.* 2000, *88(2)*, 308–316, DOI: 10.1046/j.1365-2672.2000.00969.x

29. Marchese, A.; Barbieri, R.; Coppo, E.; Orhan, I. E.; Daglia, M.; Nabavi, S. F.; Izadi, M.; Abdollahi, M.; Nabavi, S. M.; Ajami, M. Antimicrobial Activity of Eugenol and Essential Oils Containing Eugenol: A Mechanistic Viewpoint. *Crit. Rev. Microbiol.* 2017*, 43(6),* 668–689, DOI: 10.1080/1040841X.2017.1295225

30. Ulanowska, M.; Olas, B. Biological Properties and Prospects for the Application of Eugenol—A Review. *Int. J. Mol. Sci.* **2021**, *22(7)*, 3671, DOI: 10.3390/ijms22073671

31. Li, X.; Tao, Y.; Zhu, L.; Ma, S.; Luo, S.; Zhao, Z.; Sun, N.; Ge, X.; Ye, Z. Optical and Chemical Properties and Oxidative Potential of Aqueous-Phase Products from OH and $^{3}C^{*}$-Initiated Photooxidation of Eugenol. *Atmos. Chem. Phys.,* **2022**, *22*, 7793-7814. DOI :10.5194/acp-22-7793-2022.

32. Bownik, A. Clove Essential Oil from *Eugenia caryophyllus* Induces Anesthesia, Alters Swimming Performance, Heart functioning and Decreases Survival Rate During Recovery of *Daphnia magna*. *Turk. J. Fish. Aquat. Sci*. **2015**, *15(1)*, 157-166. DOI: 10.4194/1303-2712-v15_1_17

33. Ferrando, N.; Pino-Otín, M. R.; Terrado, E.; Ballestero, D.; Langa, E. Bioactivity of Eugenol: A Potential Antibiotic Adjuvant with Minimal Ecotoxicological Impact. *Int. J. Mol. Sci.* **2024**, *25(13)*, 7069, DOI: 10.3390/ijms25137069

34. Tullio, S. C. M. C.; Chalcraft, D. R. Converting Natural Nanoclay into Modified Nanoclay Augments the Toxic Effect of Natural Nanoclay on Aquatic Invertebrates. *Ecotoxicol. Environ. Saf.* **2020**, *197*, 110602, DOI: 10.1016/j.ecoenv.2020.110602

35. OECD. Test No. 211: *Daphnia magna* Reproduction Test. OECD Publishing, Paris, 2012, DOI: 10.1787/9789264185203-en

36. OECD. Test No. 202: *Daphnia* sp. Acute Immobilisation Test. OECD Publishing, Paris, 2004, DOI: 10.1787/9789264069947-en

37. Bhatt, H.B.; Baladhia, J.; Patel, R. Diffusive Light Transmission in Bentonite Colloids. *J. Opt.* **2013**, *43(3)*, 177-181. DOI: 10.1007/s12596-013-0138-9

38. Anthony, J. W.; Bideaux, R.A.; Bladh, K.W.; Nichols, M.C. Handbook of Mineralogy (version 1.2), 2001, Mineralogical Society of America. http://www.handbookofmineralogy.org/

39. Bruijning, M.; Visser, M. D.; Hallmann, C. A.; Jongejans, E. TRACKDEM: Automated particle tracking to obtain population counts and size distributions from videos in R. *Methods Ecol. Evol.* **2018**, *9(4)*, 965–973, DOI: 10.1111/2041-210X.12975

40. Rueden, C.T.; Schindelin, J.; Hiner, M.C.; DeZonia, B.E.; Walter, A.E.; Arena, E.T.; Eliceiri, K.W. ImageJ2: ImageJ for the next generation of scientific image data. *BMC Bioinformatics* **2017**, *18 (529)*, 1-26, DOI: 10.1186/s12859-017-1934-z

41. Ritz, C., Baty, F., Streibig, J. C., Gerhard, D. Dose-Response Analysis Using R. *PLoS ONE* **2015**, *10(12)*, e0146021, DOI: 10.1371/journal.pone.0146021

42. Clemente, Z.; Grillo, R.; Jonsson, M.; Santos, N. Z. P.; Feitosa, L. O., Lima, R.; Fraceto, L. F. Ecotoxicological Evaluation of Poly(ε-Caprolactone) Nanocapsules Containing Triazine Herbicides. *J. Nanosci. Nanotechnol.* **2014**, *13*, 4911–4917, DOI: 10.1166/jnn.2014.8681.

43. Blewett, T. A.; Qi, A. A.; Zhang, Y.; Weinrauch, A. M.; Blair, S. D.; Folkerts, E. J.; Sheedy, C.; Nilsson, D.; Goss, G. G. Toxicity of Nanoencapsulated Bifenthrin to Rainbow Trout (*Oncorhynchus mykiss*). *Environ. Sci. Nano* **2019**, *6(9)*, 2777–2785, DOI: 10.1039/C9EN00598F

44. Zhang, T.; Sun, H.; Hu, S.; Ding, S.; Zhang, P.; Wang, L.; Fan, W.; Liu, F.; Mu, W.; Pang, X. Self-Assembly of Eugenol-Loaded Particles to Regulate the Adhesion of Carriers on Leaves for Efficient Foliar Applications and Ecotoxicological Safety. *Ecotoxicol. Environ. Saf.* **2023**, *267*, 115602, DOI: 10.1016/j.ecoenv.2023.115602

45. EFSA. Conclusion on the Peer Review of the Pesticide Risk Assessment of the Active Substance Plant Oils/Clove Oil. *EFSA Journal* **2012**, *10(1)*, 2506, DOI: 10.2903/j.efsa.2012.2506

46. Gueretz, J. S.; Somensi, C. A.; Martins, M. L.; Souza, A. P. D. Evaluation of Eugenol Toxicity in Bioassays with Test-Organisms. *Ciência Rural* **2017**, *47(12)*, 1-5, DOI: 10.1590/0103-8478cr20170194

47. Baker, B. P.; Grant, J. A. Eugenol Profile. Active Ingredient Eligible for Minimum Risk Pesticide Use. Integrated Pest Management Program, 2018. http://hdl.handle.net/1813/56125 (accessed 2025-03-05).

48. Geller, W.; Müller, H. The Filter Apparatus of Cladocera: Filter Mesh-Sizes and their Implications on Food Selectivity. *Oecologia* **1981**, *49, 316-321.* DOI: 10.1007/BF00347591.

49. DeMott, W.R. The Influence of Prey Hardness on *Daphnia's* Selectivity for Large Prey. *Hydrobiologia,* **1995**, *307*, 127-138. DOI: 10.1007/BF00032004.

50. Reilly, K.; Ellis, L.-J. A.; Davoudi, H.H.; Supian, S.; Maia, M.T.; Silva, G.H.; Guo, Z.; Martinez, D.S.T.; Lynch, I. *Daphnia* as a Model Organism to Probe Biological Responses to Nanomaterials – from Individual to Population Effects via Adverse Outcome Pathways. *Front. Toxicol.,* 2023, *5,* 115392. DOI: 10.3389/ftox.2023.1178482.

51. Van der Zande, M.; Kokalj, A.J.; Spurgeon, D.J.; Loureiro, S.; Silva, P.V.; Khodaparast, Z.; Drobne, D.; Clark, N.J.; Van den Brink, N.W.; Baccaro, M.; Van Gestel, C.A.M.; Bouwmeester, H.; Handy, R.D. The Gut Barrier and the Fate of Engineered Nanomaterials: a View from Comparative Physiology. *Environ. Sci.: Nano,* 2020, *7*, 1974-1898. DOI: 10.1039/D0EN00174K.

52. OECD Test No. 318: Dispersion Stability of Nanomaterials in Simulated Enviromental Media. OECD Publishing, Paris, 2017, DOI: 10.1787/9789264284142-en

53. OECD Test No. 301: Ready Biodegradability. OECD Publishing, Paris, 1992, DOI: 10.1787/9789264070349-en

54. Pavlicek, A.; Zafiu, C.; Koppler, M.; Sitzwohl, F.; Gressler, S.; Ehmoser, E.-K.; Giese, B.; Part, F. *Assessing Nanocarriers for their Environmental Risks.* Presented at the Society of Environmental Toxicology and Chemistry Europe 35th Annual Meeting, Vienna, May 15, 2025.

55. Meredith, A. N.; Harper, B.; Harper, S. L. The Influence of Size on the Toxicity of an Encapsulated Pesticide: A comparison of Micron- and Nano-sized Capsules. *Environ. Int.* 2016, *86*, 68–74, DOI: 10.1016/j.envint.2015.10.012

56. Slattery, M.; Harper, B.; Harper, S. Pesticide Encapsulation at the Nanoscale Drives Changes to the Hydrophobic Partitioning and Toxicity of an Active Ingredient. *Nanomaterials* **2019**, *9(1)*, 81, DOI: 10.3390/nano9010081

755 TABLE OF CONTENTS

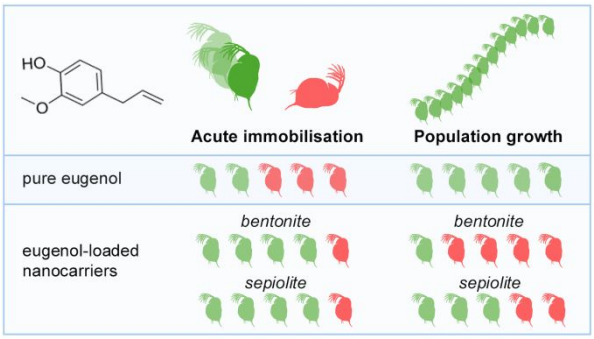

756